Flux-Line Pinning in $Bi_2Sr_2Ca_1Cu_2O_x$ Crystals: Interplay of Intrinsic 2D Behavior and Irradiation-Induced Columnar Defects

W. Gerhäuser,[1,2] G. Ries,[1] H. W. Neumüller,[1] W. Schmidt,[1] O. Eibl,[3] G. Saemann-Ischenko,[2] and S. Klaumünzer[4]

[1]*Siemens AG, Research Laboratories, Postfach 3220, W-8520 Erlangen, Federal Republic of Germany*
[2]*Physikalisches Institut, Universität Erlangen-Nürnberg, Erwin-Rommel-Strasse 1, W-8520 Erlangen, Federal Republic of Germany*
[3]*Siemens AG, Research Laboratories, Otto Hahn Ring 6, W-8000 München 83, Federal Republic of Germany*
[4]*Hahn-Meitner-Institut, Glienicker Strasse 100, W-1000 Berlin 39, Federal Republic of Germany*

(Received 31 October 1991)

We report on flux-line pinning in $Bi_2Sr_2Ca_1Cu_2O_x$ crystals by a well-defined defect structure produced through 0.5-GeV iodine irradiation. Along their path these ions create columnar damage tracks of 5 to 10 nm in diameter. Even when flux lines are aligned parallel to these tracks, the measured activation energies at low temperatures and small fields do not exceed 70 meV and the critical currents decline rapidly with increasing temperature. The small pinning energies are explained quantitatively by pinning of two-dimensional pancake vortices instead of complete flux lines.

PACS numbers: 74.70.Vy, 74.60.Ge, 74.60.Jg

One of the striking features of the high-temperature superconductors is the large superconducting anisotropy [1]. In the Bi-based materials this effect is especially pronounced due to the large distance between the CuO_2 layers compared to the coherence length ξ_c. Theories assuming two-dimensional superconducting layers separated by insulating material [2] lead to the idea of pancake vortices [3]. This model has important implications for the mechanism of flux-line pinning, and its validity for the Bi-based compounds leads consequently to drastic constraints in technical applications at liquid-nitrogen temperatures. In this Letter this model will be tested by the determination of the interaction volume between defect and vortex. For this purpose we introduced very anisotropic line defects as pinning centers in the $Bi_2Sr_2Ca_1Cu_2O_x$ compound using 0.5-GeV iodine ions to create amorphous tracks along their paths through the material [4]. Previous experiments on both polycrystalline material and single crystals using oxygen ions [5] and neutrons [6] yielded an increase in critical current, but no change in the pinning energy was observed in the polycrystalline material, although these particles produced a spectrum of defects ranging from Frenkel pairs to large clusters. High-energy heavy-ion irradiation experiments were mainly performed on Y-Ba-Cu-O material: Xe or Pb on thin films [7–9] and single crystals [10]. The recent results of Civale *et al.* [11], using Sn ions, demonstrated an increase of both the irreversibility line and the critical currents. But according to Clem [3] Y-Ba-Cu-O is not the appropriate material to test the pancake model because of its significantly lower anisotropy. In the Bi and Tl system few data exist up to now [12–14].

For irradiation, $Bi_2Sr_2Ca_1Cu_2O_x$ single crystals were grown from the melt using Al_2O_3 crucibles [6]. The crystals had typical dimensions up to $2\times2\times(0.02\text{–}0.1)$ mm^3. Thin crystal sheets of thickness $d=5\text{–}14$ μm were obtained by cleavage of thicker crystals and cut to dimensions of approximately 1×1 mm^2. The critical temperatures before irradiation, measured by ac susceptibility, range from $T=80$ to 86 K with transition widths of $\Delta T=1\text{–}4$ K.

The irradiation was done at the low-temperature facility of VICKSI at the Hahn-Meitner-Institut in Berlin at a temperature of approximately 70 K. Afterwards, the samples were warmed up to room temperature. As projectiles we used 0.5-GeV ^{127}I ions which have a projected range of about 27 μm in $Bi_2Sr_2Ca_1Cu_2O_x$; the electronic energy loss varies by less than 20% within the sample thickness. The direction of the ion beam was parallel to the c axis. In order to confirm the columnar defect structure, an irradiated crystal (dose $\phi t=5\times10^{10}$ ions/cm^2) was prepared for transmission electron microscopy (TEM) analysis. Figure 1 shows a TEM high-resolution

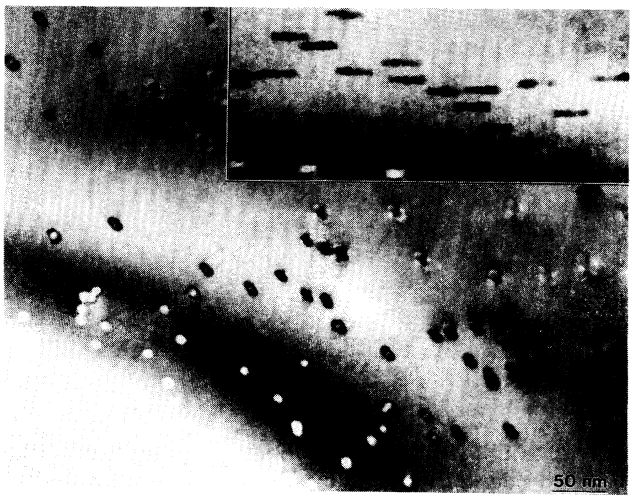

FIG. 1. TEM image of an irradiated cyrstal (dose 5×10^{10} ions/cm^2) with the view direction parallel to the ion tracks. Inset: The same region under a tilt angle of 20°.

image with the electron beam parallel to the ion tracks. Disks with a diameter of 5–10 nm are observed with a density that corresponds directly to the applied dose. The inset of Fig. 1 shows the same region imaged under a tilt angle of 20°, verifying that the ion-induced defects are indeed continuous cylinders. The damaged region was not analyzed in detail but might be amorphous.

A number of crystals were irradiated with different doses $\phi t = 2\times10^{10}$, 5×10^{10}, 1×10^{11}, 1.5×10^{11}, and 2.5×10^{11} ions/cm^2. The reduction of the critical temperature was nearly linear with a slope of $\Delta T_c/\phi t = 2.6\times10^{-11}$ K(ions/cm^2)$^{-1}$. In the further discussion it will be useful to express the dose as dose-equivalent field value, $B_\phi = \Phi_0\phi t$ (Φ_0 is the elementary flux quantum). At $B = B_\phi$ the density of vortices just equals the density of ion tracks. The applied doses correspond to 0.4, 1, 2, 3.1, and 5.2 T, respectively.

Critical currents were determined magnetically using a commercial SHE SQUID magnetometer. Figure 2(a) shows the magnetization current density j_{cm} at $T = 10$ K derived from the width of the magnetization loop ΔM using the Bean model [15]: $j_{cm} = 3\Delta M/\mu_0 D$ (D is the average diameter of the crystal). The field is applied parallel to the c axis and therefore parallel to the ion tracks. There is a marked enhancement of j_{cm} due to the additionally generated pinning centers. It is surprising that the values of j_{cm} at low fields $B < 0.5B_\phi$ are close to those measured at 5 K in Sn-irradiated Y-Ba-Cu-O [11] at corresponding ion doses and in the same range as obtained for epitaxially grown thin films of Y-Ba-Cu-O [7] and $Bi_2Sr_2Ca_1Cu_2O_x$ [1]. With increasing field j_{cm} decreases faster in Bi-Sr-Ca-Cu-O than in Y-Ba-Cu-O.

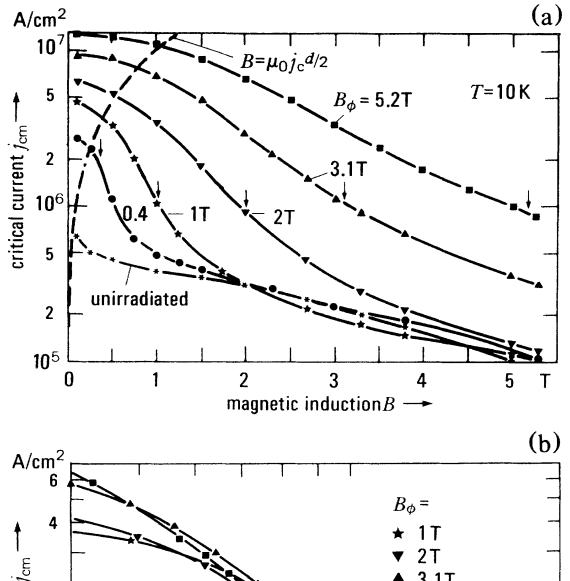

FIG. 2. (a) Magnetization currents j_{cm} vs the applied magnetic induction $B_{\|c}$ before and after iodine irradiation at $T = 10$ K. The arrows indicate the dose where $B = B_\phi$. In the region left of the dotted line the self-field exceeds the applied field (see text). (b) The same data vs the normalized field B/B_ϕ exhibiting a universal $j_c \propto B^{-2}$ behavior.

We note that the field range of j_c enhancement grows with the applied dose. This becomes even more evident in Fig. 2(b) where j_{cm} is plotted versus the rescaled field B/B_ϕ. For $0.5B_\phi \leq B \leq 2B_\phi$ the critical current closely follows a universal curve with $j_c \propto B^{-2}$ for all doses investigated. We take this as strong evidence that B/B_ϕ, which is just the average number of vortices per ion track, is the relevant parameter to determine the volume pinning force. For high fields $B > B_\phi$ there must remain an excess number of vortices which can only interact with the pinning centers present in the crystal prior to irradiation. Consequently, j_{cm} approaches, for $B \gtrsim 2B_\phi$, the exponential $j_c(B)$ curve ("scaling law" [16]) for zero dose. In contrast, at low fields each flux line is pinned by an ion track and j_{cm} exhibits a weaker field dependence as long as $B < B_\phi/2$. In the low-field regime we must take into account the role of the self-field, too. The magnetization currents in the disk-shaped samples generate both radial and axial self-field components of the order of $\mu_0 j_{cm} d/2$ [17], where $d = 10$ μm is a typical sample thickness. In the region left of the dashed line in Fig. 2(a) the self-field exceeds the applied field and controls the $j_c(B)$ behavior. Above 10 K the critical currents decline rapidly. At $T = 60$ K, j_{cm} decreases after irradiation from 5×10^3 A/cm^2 at $B = 0$ T by 1 order of magnitude in a field of 0.1–0.15 T. No correlation with the dose is observed. This result is in striking contrast to the observations on Sn-irradiated Y-Ba-Cu-O crystals [11] where j_{cm} increases with the dose and is enhanced to some 10^5 A/cm^2 at 77 K even in fields of some teslas. According to TEM analysis the nature and desity of the defects at equal doses of Sn and iodine ions are similar. Therefore, this discrepancy has to be attributed to the large difference in the anisotropy of these two materials.

For a closer investigation of the pinning process, we measured the magnetization decay $M(t)$. Effective activation energies $U(B,\phi t)$ were evaluated using $U = k_B T[S^{-1} + \ln(t_b/\tau)]$ [18], where $S = [1/M(t_b)] \times dM(t)/d\ln t$ is the logarithmic slope derived from the $M(t)$ curve, t_b is the time of the first measurement after field settlement ($t_b \approx 100$ s), and τ is an *a priori* unknown relaxation time. We used a reasonable value of $\tau = 10^{-10}$ s. Figure 3 shows U at $T = 10$ K as a function of the ion dose for different field values. In the unirradiated state U has an intrinsic value of 30–35 meV. As a result of the heavy-ion-induced defect structure, U in-

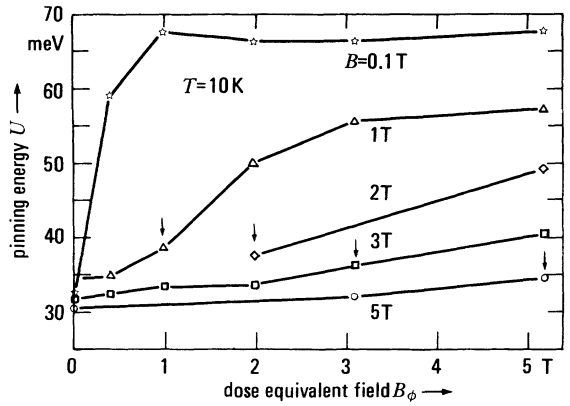

FIG. 3. Pinning energies U vs the dose-equivalent field B_ϕ at various magnetic inductions B. The arrows indicate the dose where $B = B_\phi$.

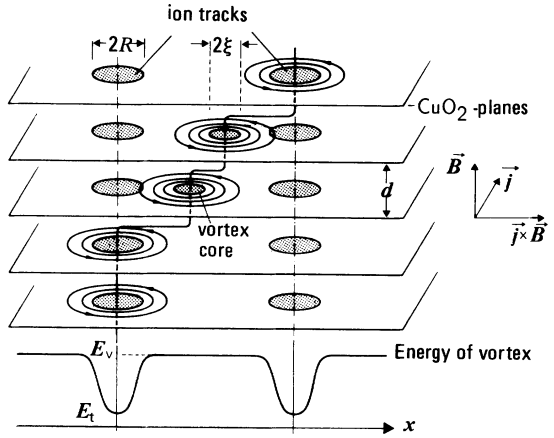

FIG. 4. Schematic picture of vortex pinning on an ion track in CuO_2 planes.

creases markedly, similar to $j_{cm}(B)$. The effect on U remains small as long as $B > B_\phi$, i.e., the number of defects is less than the number of vortices. In this "saturated" case flux creep is controlled by thermal activation of the unbound excess vortices which interact with the intrinsic defects in the crystal. In the intermediate region U varies roughly with $1/B$. Only for an appropriate majority of defects, i.e., $B_\phi > 2B$, does U saturate at a level which is significant for the interaction between vortex and ion track.

Because after heavy-ion irradiation one type of defect is predominant, it is tempting to interpret our results within a microscopic picture of the defect-vortex interaction. We start with Clem's pancake-vortex model [3] for which the shielding currents, circulating around the normal-conducting vortex core, are restricted to the copper oxide double planes. The energy of such a pancake vortex is the sum of the core energy E_c plus the energy E_e of the magnetic field and supercurrents [19]:

$$E_v = E_c + E_e = \frac{\mu_0}{2} H_c^2 \pi \xi_{ab}^2 d + \frac{\Phi_0^2 d}{\mu_0 4\pi \lambda_{ab}^2} \ln \frac{\lambda_{ab}}{\xi_{ab}} . \quad (1)$$

Here $d = 1.5$ nm is the separation between the CuO_2 planes, $\mu_0 H_c \approx 1$ T the thermodynamic critical field, $\xi_{ab} = 1.8$ nm the coherence length, and $\lambda_{ab} = 270$ nm the London penetration depth. We regard an ion track as a stack of presumably normal-conducting disks with diameter $2R = 10$ nm (see Fig. 4). For a trapped vortex the radius of the inner edge of the current system is now R instead of ξ_{ab} and the vortex energy is reduced to $E_l = (\Phi_0^2 d/\mu_0 4\pi\lambda_{ab}^2) \ln(\lambda_{ab}/R)$. Therefore, the pinning energy of one pancake vortex is

$$U = E_v - E_l = E_c + \frac{\Phi_0^2 d}{\mu_0 4\pi \lambda_{ab}^2} \ln \frac{R}{\xi_{ab}} . \quad (2)$$

With the material parameters listed above we obtain $E_c \approx 35$ meV and $U \approx 70$ meV. This is just what we observe as saturation value U at 10 K and $B = 0.1$ T. We argue that this low-field limit is the unmasked interaction as in this case the average distance between vortices is of the order of λ_{ab}, so that they may be regarded as fairly isolated.

This success of the pancake pinning model has important implications regarding the general nature of the depinning process under Lorentz forces in the $Bi_2Sr_2Ca_1$-Cu_2O_x compound. The field applied parallel to the columnar defects should be the most favorable situation for pinning. Even if we take into account that vortices are curved due to the transverse self-field component, the interacting length between a bent vortex and a straight defect should comprise many CuO_2 layers. The total binding energy is the sum of the single-pancake interactions [Eq. (2)] and therefore may well be many electronvolts. This is in sharp contrast to our flux-creep results which state that the single-pancake–defect interaction determines the effective activation energy. Obviously thermally activated depinning of a pinned vortex does not occur as one single event but in a stepwise manner as a sequence of liberations of individual pancake vortices. Figure 4 visualizes this process. This basic depinning process may occur at random positions along the vortex or perhaps in a ziplike manner, until the flux line has entirely moved to the next pinned position. As becomes evident regarding Fig. 4, this mode of depinning inevitably implies a considerable amount of shear between the pancake vortices in adjacent planes. To be energetically favorable, the associated elastic shear force must be less than the pancake pinning force. Indeed, elasticity theories [3,20] for the vortex lattice in a layered superconductor predict an enormous reduction of the relevant tilt modulus c_{44} by a factor of $(\lambda_{ab}/d)^2 \sim 10^4$ compared to the bulk value in an isotropic superconductor. This applies for a strongly anisotropic material like $Bi_2Sr_2Ca_1$-Cu_2O_x with mainly magnetic coupling between the pancake vortices. In the much less anisotropic Y-Ba-Cu-O

the coupling of adjacent CuO_2 layers is stronger. A thermal activation process may include several pancakes with an accordingly larger activation threshold and less reduction of j_c by flux creep at elevated temperatures.

As a further test of this picture of the elementary pinning mechanism after heavy-ion irradiation it is interesting to estimate the critical current to be expected. To get an upper limit we assume that each pancake vortex is trapped by an ion track. This is the case in the low-field limit $B \ll B_\phi$ where direct summation of the individual forces to a volume pinning force is appropriate. At $T=10$ K and $B=0.1$ T the factor U/kT is about 80. This means that j_{cm} after 100 s did not decay too much below the depinning critical current $j_{c0} \approx (U/R)/\phi_0 d$. With the data given above we get an estimated upper limit $j_{c0} \approx 7\times10^7$ A/cm^2. This calculated j_c is about a factor of 5 larger than the observed low-field values obtained in the heavily irradiated crystals. The difference might be due to flux-creep effects or to uncertainties in the effective radius R. A further uncertainty arises from the influence of the self-fields.

In summary, we have produced a well-defined columnar damage structure in $Bi_2Sr_2Ca_1Cu_2O_x$ crystals by heavy-ion irradiation. After irradiation we found in the field region $B_\phi/2 < B < 2B_\phi$ a universal $j_c \propto B^{-2}$ behavior. The enhancement of j_c and U at low temperatures and fields can be understood quantitatively applying Clem's pancake model. We found evidence that depinning occurs as thermally activated hopping of single pancake vortices in a CuO_2 double layer. Efforts should be directed towards materials with a larger number of CuO_2 layers which enhance the energy of a single pancake vortex accordingly or towards improving the interlayer coupling so that the vortices act merely as coherent linear objects like in isotropic superconductors.

We thank M. Kraus for his help at the HMI as well as R. Busch for helpful discussions.

[1] P. Schmitt, P. Kummeth, L. Schulz, and G. Saemann-Ischenko, Phys. Rev. Lett. **67**, 267 (1991).

[2] W. E. Lawrence and S. Doniach, in *Proceedings of the Twelfth International Conference on Low Temperature Physics, Kyoto, 1970*, edited by E. Kanda (Keigaku, Tokyo, 1971), p. 361.

[3] J. R. Clem, Phys. Rev. B **43**, 7837 (1991).

[4] B. Hensel, B. Roas, S. Henke, R. Hopfengärtner, M. Lippert, J. P. Ströbel, M. Vildic, G. Saemann-Ischenko, and S. Klaumünzer, Phys. Rev. B **42**, 4135 (1990).

[5] H. W. Neumüller, G. Ries, W. Schmidt, W. Gerhäuser, and S. Klaumünzer, J. Less-Common Met. **164&165**, 1351 (1990); Supercond. Sci. Technol. **4**, 370 (1991).

[6] W. Gerhäuser, H. W. Neumüller, W. Schmidt, G. Ries, G. Saemann-Ischenko, H. Gerstenberg, and F. M. Sauerzopf, in Proceedings of M^{2}S-HTSC III, Kanazawa, Japan, 1991 [Physica (Amsterdam) C (to be published)].

[7] B. Roas, B. Hensel, S. Henke, S. Klaumünzer, B. Kabius, W. Watanabe, G. Saemann-Ischenko, L. Schultz, and K. Urban, Europhys. Lett. **11**, 669 (1990).

[8] G. Kreiselmeyer, B. Hensel, G. Saemann-Ischenko, D. Groult, J. Provost, and S. Bouffard (to be published).

[9] H. Watanabe, B. Kabius, K. Urban, B. Roas, S. Klaumünzer, and G. Saemann-Ischenko, Physica (Amsterdam) **179C**, 75 (1991).

[10] F. Rullier-Albenque, A. Legris, S. Bouffard, E. Paumier, and P. Lejay, Physica (Amsterdam) **175C**, 111 (1991).

[11] L. Civale, A. D. Marvick, T. K. Worthington, M. A. Kirk, J. R. Thompson, L. Krusin-Elbaum, Y. Sun, J. R. Clem, and F. Holtzberg, Phys. Rev. Lett. **67**, 648 (1991).

[12] W. Gerhäuser, H. W. Neumüller, W. Schmidt, G. Ries, O. Eibl, G. Saemann-Ischenko, and S. Klaumünzer, in Proceedings of M^{2}S-HTSC III (Ref. [6]).

[13] H. Watanabe, B. Kabius, K. Urban, S. Klaumünzer, P. Schmitt, and G. Saemann-Ischenko, in Proceedings of M^{2}S-HTSC III (Ref. [6]).

[14] V. Hardy, D. Groult, J. Provost, M. Hervieu, B. Raveau, and S. Bouffard, Physica (Amsterdam) **178C**, 255 (1991).

[15] C. P. Bean, Phys. Rev. Lett. **8**, 250 (1962).

[16] H. W. Neumüller and G. Ries, Physica (Amsterdam) **160C**, 471 (1989).

[17] M. Daeumling and D. C. Larbalestier, Phys. Rev. B **40**, 9350 (1989).

[18] M. R. Beasley, R. Labusch, and W. W. Webb, Phys. Rev. **181**, 682 (1969).

[19] H. Ullmaier, *Irreversible Properties of Type II Superconductors* (Springer, Berlin, 1975).

[20] A. Sudbø and E. H. Brandt, Phys. Rev. Lett. **66**, 1781 (1991).

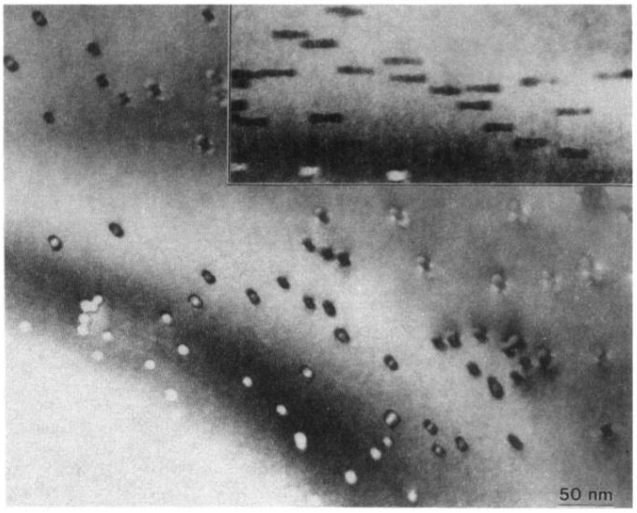

FIG. 1. TEM image of an irradiated cyrstal (dose 5×10^{10} ions/cm^2) with the view direction parallel to the ion tracks. Inset: The same region under a tilt angle of 20°.

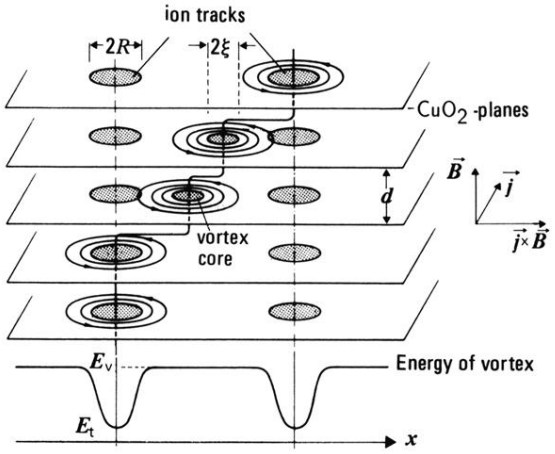

FIG. 4. Schematic picture of vortex pinning on an ion track in CuO_2 planes.